Cyclic Nucleotide-gated Channels on the Flagellum Control Ca^{2+} Entry into Sperm

Burkhard Wiesner,* Jocelyn Weiner,‡ Ralf Middendorff,§ Volker Hagen,* U. Benjamin Kaupp,‡ and Ingo Weyand‡

*Forschungsinstitut für Molekulare Pharmakologie, D-10315 Berlin; ‡Institut für Biologische Informationsverarbeitung, Forschungszentrum Jülich, D-52425 Jülich; and §Anatomisches Institut, Universitätskrankenhaus Eppendorf, D-20246 Hamburg

Abstract. Cyclic nucleotide-gated (CNG) channels are key elements of cGMP- and cAMP-signaling pathways in vertebrate photoreceptor cells and in olfactory sensory neurons, respectively. These channels form heterooligomeric complexes composed of at least two distinct subunits (α and β). The α subunit of cone photoreceptors is also present in mammalian sperm. Here we identify one short and several long less abundant transcripts of β subunits in testis. The α and β subunits are expressed in a characteristic temporal and spatial pattern in sperm and precursor cells. In mature sperm, the α subunit is observed along the entire flagellum, whereas the short β subunit is restricted to the principal piece of the flagellum. These findings suggest that different forms of CNG channels coexist in the flagellum. Confocal microscopy in conjunction with the Ca^{2+} indicator Fluo-3 shows that the CNG channels serve as a Ca^{2+} entry pathway that responds more sensitively to cGMP than to cAMP. Assuming that CNG channel subtypes differ in their Ca^{2+} permeability, dissimilar localization of α and β subunits may give rise to a pattern of Ca^{2+} microdomains along the flagellum, thereby providing the structural basis for control of flagellar bending waves.

Key words: signal transduction • cGMP • fertilization • chemotaxis • caged compounds

GAMETES use chemoattractive factors to increase the probability of sperm–egg interaction (for review see Ward and Kopf, 1993). Sperm chemoattraction is well-established in species with external fertilization. In sea urchin, the best-studied species, several lines of evidence suggest that cyclic nucleotides and Ca^{2+} control sperm chemoattraction (Garbers, 1989). Peptides secreted from sea urchin eggs bind to membrane receptors of sperm, thereby increasing the intracellular concentrations of cyclic nucleotides and Ca^{2+} (Hansbrough and Garbers, 1981; Schackmann and Chock, 1986). A rise of the intracellular Ca^{2+} concentration ($[Ca^{2+}]_i$) has been proposed to alter sperm motility (Ward et al., 1985; Cook et al., 1994). However, the control mechanism(s) of swimming behavior, the site(s) of Ca^{2+} entry into sperm, and the molecular identity of the Ca^{2+} conductance remain unknown.

In contrast to species with external fertilization, evidence is sparse for chemoattraction of sperm in mammals. Studies in mammals are complicated by the process of capacitation (Cohen-Dayag et al., 1995). Furthermore, sperm migration within the female genital tract may be controlled not only by factors secreted by the egg, but also by factors in the follicular fluid (Ralt et al., 1991; Cohen-Dayag et al., 1995) or the oviduct (for review see Harper, 1994). Whether chemoattraction of mammalian sperm is mediated by signaling pathways involving cyclic nucleotides and Ca^{2+} is not known.

Recently, a cyclic nucleotide-gated (CNG)[1] channel was identified in mammalian sperm (Weyand et al., 1994). CNG channels are directly opened by either cAMP or cGMP, and are permeable to Ca^{2+} ions (for review see Kaupp, 1995; Finn et al., 1996). By virtue of their high Ca^{2+} permeability (Frings et al., 1995), CNG channels are prime candidates for mediating Ca^{2+} entry into sperm that is controlled by cyclic nucleotides. CNG channels form heterooligomeric complexes composed of homologous α and β subunits (for review see Kaupp, 1995; Finn et al., 1996). When heterologously expressed, the α subunits form functional channels on their own, whereas β subunits alone are not functionally active. Coexpression of α and β

Burkhard Wiesner and Jocelyn Weiner contributed equally to this work.

Address all correspondence to Dr. I. Weyand, IBI, Forschungszentrum Jülich, 52425 Jülich, Germany. Tel.: 49-2461-614040; Fax: 49-2461-614216; E-mail: i.weyand@fz-juelich.de

1. *Abbreviations used in this paper*: aa, amino acid residue; CNC, cyclic nucleotide-gated channel; CNG, cyclic nucleotide-gated; DMNB, 4,5-dimethoxy-2-nitrobenzyl; GARP, glutamic acid-rich protein; MCM, (7-methoxy-coumarin-4-yl)methyl.

subunits results in channel species that differ from homooligomeric channels in several properties such as ligand sensitivity, ligand selectivity, and interaction with Ca^{2+} ions (Chen et al., 1993; Bradley et al., 1994; Liman and Buck, 1994; Körschen et al., 1995; Gordon et al., 1996; Sautter et al., 1998; Bönigk, Sesti, Bradley, Ronnett, Müller, Kaupp, and Frings, manuscript submitted for publication). The homooligomeric α subunit cloned from bovine testis responds roughly 200-fold more sensitive to cGMP than to cAMP (Weyand et al., 1994), suggesting that the channel represents the target of a cGMP-signaling pathway.

In sperm from both vertebrates and invertebrates, several cellular processes (e.g., acrosomal exocytosis) are regulated by cyclic nucleotides and $[Ca^{2+}]_i$ (Santos-Sacchi and Gordon, 1980; Arnoult et al., 1996; Rotem et al., 1998). Therefore, CNG channels may subserve several functions including chemoattraction and exocytosis.

We set out to study the physiological role(s) of CNG channels in sperm by determining their molecular composition and their expression pattern. Our experiments provide evidence for a short and several long less abundant transcripts of β subunits in testis. The short β subunit variant is expressed in sperm. In mature sperm, α and β subunits have different but overlapping spatial distributions along the flagellum. We show that activation of flagellar CNG channels increases $[Ca^{2+}]_i$ of sperm. The CNG channel–mediated Ca^{2+} influx is more sensitive to cGMP than to cAMP. The localization on the flagellum strengthens the idea that Ca^{2+} entry through CNG channels controls sperm motility. The distinct regional expression of channel subtypes along the flagellum might produce a spatiotemporal profile of Ca^{2+} concentrations that may underlie complex flagellar beating patterns.

Materials and Methods

We will use a nomenclature for CNG channels that describes the subunit type (α, β) and the channel subfamily (1, 2, 3). In vertebrates, three distinct genes encoding α subunits have been identified. The respective gene products have been originally identified either in rod (1) or in cone (2) photoreceptors, or in olfactory sensory neurons (3); alternatively spliced variants are indicated by small letters. A preceding p (for plasmid) indicates the respective cDNA sequence.

Preparation of RNA and Construction of cDNA Library

Bovine testicular tissue and retinae were frozen immediately in liquid nitrogen at the abattoir. Poly(A)$^+$ RNA was isolated using the guanidinium isothiocyanate method (Chirgwin et al., 1979), followed by a cesium-trifluoroacetic acid gradient and oligo(dT)-cellulose chromatography (Aviv and Leder, 1972). First-strand cDNA was synthesized with M-MLV reverse transcriptase (Life Technologies, Eggenstein, Germany) using oligo$(dT)_{17}$ or random hexamers as primer. Primers were removed by filtration on a Centricon-100 spin column (Amicon Corp., Easton, TX). A random-primed cDNA library was constructed from bovine testis poly(A)$^+$ RNA in λZAP II vector (Stratagene, La Jolla, CA).

Isolation and Characterization of cDNA Clones

Degenerate primers corresponding to amino acid (aa) sequences KYMAFFE (aa 882–888) and QMIFD (aa 1083–1087) of the CNG channel β subunit from bovine rods (CNCβ1a; Körschen et al., 1995) were used to amplify a fragment from bovine testis first-strand cDNA. The PCR fragment was used to screen an oligo(dT)-primed testis cDNA library (Weyand et al., 1994). The longest clone thus isolated contained nucleotides 1319–3061 of the final clone pCNCβ1c (see Results, Fig. 2 *a*). The sequence was identical to the corresponding sequence of CNCβ1a (Körschen et al., 1995). Subsequently, a random-primed cDNA library was screened with a cDNA probe of CNCβ1a (corresponding to nucleotides 1193–1798 of pCNCβ1c). The longest clone thus isolated carried nucleotides 1138–2916 of pCNCβ1c. The combined sequence of the partial clones (pCNCβP) did not harbor the complete coding region (see Fig. 1 *a*). Because cDNA sequences were identical with the corresponding sequences of CNCβ1a, the 5′ end of testis β cDNA was probed by PCR using primers derived from the CNCβ1a sequence (for positions of primers, see Fig. 1 *a*). cDNA from bovine retina was used as control for amplification. The initial primer set consisted of primer 1 (GGATGGATTCCAGGCGG; inverse complement of nucleotides 1305–1321 of pCNCβ1c) as the 3′ primer and primer 2 (TGCTCTGCTGCAAGTTCAAA; nucleotides 860–879) or primer 3 (GAACTGCAGGTGGAAGAC; nucleotides 370–387) as 5′ primers. A set of nested primers consisted of primer 4 (GGCGTTTGAACTTGCAGC; inverse complement of nucleotides 866–883) as 3′ primer, and primer 5 (AGCTCATCGACCCTGACG; nucleotides 728–745), primer 6 (GCAACCTCGACAGCCAGC; nucleotides 631–648), or primer 7 (CTCAAGATGCTGTCACCG; nucleotides 547–564) as 5′ primers. For blot hybridization, PCR fragments were hybridized under high-stringency conditions (5× SSC, 5× Denhardt's, 0.1 mg/ml denatured herring testis DNA, 0.1% SDS, 65°C) with ^{32}P-labeled DNA probes (~10^6 cpm/ml). Filters were washed with 1× SSC, 0.1% SDS at 65°C (2 × 30 min).

The PCR analysis demonstrated that short and long β transcripts are expressed in testis. The 5′ ends of the long β cDNAs were isolated by modification of the rapid amplification of cDNA ends (RACE) technique (Frohman et al., 1988). Random-primed cDNA was (dA)-tailed. PCR was carried out with the gene-specific primer R (CTTGGGGCTCTCCTCATCGG, inverse complement of nucleotides 752–771 of pCNCβ1c; for the location of primer R, see Fig. 1 *a*), the hybrid adapter primer GACTCGAGTCGACATCGA$(T)_{17}$, and the adapter primer GACTCGAGTCGACATCGA. To enrich the desired PCR product, a second PCR was carried out on the first PCR product using a nested gene-specific primer (TTCCTGAGGCTCCCTGTGG; inverse complement of nucleotides 494–512 of pCNCβ1c), and the adapter primer. PCR fragments >150 bp were cloned into pBluescript SK-vector. Colonies were hybridized with a DNA probe amplified with two primers (GAACTGCAGGTGGAAGAC, nucleotides 370–387 of pCNCβ1c; TTCCTGAGGCTCCCTGTGG, inverse complement of nucleotides 494–512) using cDNA of CNCβ1a as template. We obtained several clones with three distinct 5′ ends: pCNCβ1c (seven clones), pCNCβ1d (two clones), and pCNCβ1e (three clones).

Attempts to clone the 5′ end of the short β cDNA (CNCβ1f) by screening cDNA libraries were not successful. The PCR analysis, however, indicated that the short β cDNA begins in the segment flanked by primers 5 and 6.

Northern Blot Analysis

A blot with poly(A)$^+$ RNA from bovine testis (6 μg) and retina (10 μg) was hybridized under high-stringency conditions (50% formamide, 5× SSC, 5× Denhardt′s, 0.1 mg/ml denatured herring testis DNA, 0.1% SDS, 65°C) with ^{32}P-labeled riboprobes. Filters were washed with 1× SSC, 0.1% SDS at 65°C (2 × 30 min).

Polyclonal Antibodies Against CNG Channel Subunits

Polyclonal antibody FPc 21K is directed against the NH_2-terminal domain (aa 574–763) of the β′ part of CNCβ1a (Körschen et al., 1995), whereas polyclonal antibody PPc 32K is directed against an epitope (aa 1292–1334) close to the COOH terminus of CNCβ1a. Polyclonal antibody PPc 23 was raised against the COOH-terminal domain (aa 593–706) of the α subunit of the bovine cone CNG channel (CNCα2; Weyand et al., 1994). Polyclonal antibodies were purified from rabbit serum by affinity chromatography on a column consisting of the respective antigen (3–5 mg) coupled to activated CH-Sepharose 4B (Pharmacia Biotech, Inc., Piscataway, NJ). The antibody was eluted with 0.1 M glycine HCl, pH 2.5, immediately neutralized with 1/8 vol 1 M Tris HCl, pH 8.0, and dialyzed against PBS. Purified antibodies were concentrated using a Centricon-100 spin column (Amicon Corp.) and stored at –80°C in the presence of 50% glycerol, 0.2 mg/ml BSA, 0.1% NaN_3. The specificity of the antibodies in immunohistochemistry was tested on cryosections of bovine retina.

Western Blot Analysis

For transient expression, cDNAs for the short testis β subunit (CNCβ1f) and one of the long β subunits (CNCβ1c) were cloned into pcDNAI vec-

tor (Invitrogen Corp., Carlsbad, CA). COS-1 cells were transfected by a modified calcium phosphate coprecipitation method (Chen and Okayama, 1987). Transfected COS-1 cells, bovine sperm, and testicular tissue were homogenized in 10 mM Hepes, pH 7.5 (NaOH), 10 mM NaCl, 1 mM DTT, 0.1 mM EGTA, 5 μg/ml aprotinin, 5 μg/ml leupeptin, 1 μg/ml pepstatin, 500 μg/ml PEFABLOC, and 10 mM benzamidine (buffer A). The suspension was centrifuged at 100,000 *g* for 20 min (4°C). The membrane pellet was resuspended in buffer A containing 500 mM NaCl, washed by centrifugation, resuspended in buffer A containing 100 mM NaCl, and 0.8% *N*-dodecylmaltoside, and left on ice for 15 min. Insoluble material was separated from solubilized membrane proteins by centrifugation (8,000 *g*, 10 min, 4°C). Membranes of bovine rod outer segments were washed two times with buffer A. Membrane proteins were separated by SDS-PAGE, transferred to Immobilon-P membrane (Millipore Corp., Bedford, MA), and sequentially probed with primary antibodies and secondary HRP-coupled goat anti-rabbit antibody for enhanced chemiluminescence detection (Amersham Corp., Arlington Heights, IL).

Immunocytochemistry

Testicular and epididymal tissue. Tissue blocks of bovine testes and epididymes were fixed in Bouin's fluid for 24 h at 20°C. Subsequently, blocks were embedded in paraffin; 6-μm sections were cut and mounted on chrome-gelatine precoated slides. Immunoreactivity was tested using a combination of the peroxidase-antiperoxidase (PAP) technique and the avidin-biotin-peroxidase complex (ABC) method (Middendorff et al., 1996). Sections were incubated for 24 h at 4°C with the primary antibodies PPc 23 (0.3–3 μg/ml), FPc 21K (1–10 μg/ml), or PPc 32K (0.06–0.9 μg/ml) diluted in PBS, 0.2% BSA, 0.25% Triton X-100, 0.1% NaN_3. Peroxidase activity was visualized by the nickel glucose oxidase technique (Záborsky and Léránth, 1985) with DAB as chromogen.

Sperm. Cauda epididymal sperm and ejaculated sperm were fixed on glass slides for 10 min with 4% paraformaldehyde, PBS, and were then washed twice with PBS. Cells were preincubated with PBS, 0.1% BSA, 1% Triton X-100, and 0.1% Tween-20 (30 min), and were then incubated overnight at 4°C with the primary antibody diluted in preincubation solution (PPc 23: 1–3 μg/ml; FPc 21K: 1–10 μg/ml; PPc 32K: 0.3–0.6 μg/ml). Cells were washed three times and incubated for 3 h with secondary goat anti–rabbit antibody coupled to a carboxymethylindocyanine dye (CY3) diluted 1:1,000 (1.5 μg/ml) in PBS, 2% FCS, 0.1% BSA, 1% Triton X-100, 0.1% Tween-20. After washing three times, cells were coverslipped in Moviol and examined by fluorescence microscopy.

Controls. Experiments were performed in the absence of primary (and in the case of tissue sections also of secondary or tertiary) antibodies. For control of specificity, primary antibodies were preadsorbed with an 80-fold molar excess of the respective immunogenic or an unrelated antigen.

Ca^{2+} Imaging Experiments

Pretreatment of sperm. Cryoconserved ejaculated bovine sperm were thawed (45 s, 37°C), diluted 10-fold with 200 mM Tris, 55 mM glucose, 65 mM citric acid monohydrate, pH 7.2 (NaOH), and washed twice by centrifugation (830 *g*, 4 min, room temperature). Sperm were resuspended in buffer B (140 mM NaCl, 4.6 mM KCl, 2 mM $CaCl_2$, 10 mM glucose, 10 mM Hepes, pH 7.4 (NaOH), checked for motility (~60% progressive motile cells), and then loaded in the dark for 30 min with the cell-permeant acetomethoxy ester of Fluo-3 (4.4×10^{-6} M in the presence of 0.01% Pluronic F-127; Molecular Probes, Inc., Eugene, OR). Sperm were centrifuged, washed (buffer B; 830 *g*, 4 min, room temperature), resuspended in buffer B, and then put on coverslips. After 5 min, buffer B was carefully aspirated, and sperm were incubated (10 min) with the respective incubation solution containing the membrane-permeable caged cyclic nucleotide analogue (see below). Incubation solutions were: buffer B, buffer B with additives (see Results), or buffer B with 500 μM EGTA instead of 2 mM $CaCl_2$.

Ca^{2+} imaging. Ca^{2+}-dependent changes in fluorescence intensity of Fluo-3 were detected with a confocal laser scanning microscope LSM 410 invert (Zeiss GmbH, Jena, Germany) using an oil immersion lens (100/1.3). Fluo-3 was excited with an argon–krypton laser (488 nm; Melles Griot, Carlsbad, CA). Fluorescence was measured at wavelengths >515 nm. For beam-splitting, a dichroic mirror FT 510 and a cutoff filter LP 515 in front of the detector unit were used.

For flash photolysis experiments, lyophilized 4,5-dimethoxy-2-nitrobenzyl (DMNB) 8-pCPT-cGMP (axial isomer), (7-methoxy-coumarin-4-yl)methyl (MCM) 8-Br-cGMP (axial isomer), and MCM 8-Br-cAMP (axial isomer) were dissolved in DMSO and then diluted in the respective incubation solution to the desired final concentration. The final DMSO concentration (maximally 2%) had no detectable effect on the fluorescence intensity of sperm. Synthesis and photochemical properties of the caged compounds will be described elsewhere. Due to its limited solubility in aqueous solutions, DMNB 8-pCPT-cGMP was used at concentrations ≤50 μM.

DMNB 8-pCPT-cGMP was photolyzed with a continuous argon-ion laser (364 nm; Spectra-Physics, Darmstadt, Germany) that allowed local UV irradiation of sperm. Therefore, UV-induced bleaching of Fluo-3 is restricted to the illuminated region, and thus does not compromise determination of the Ca^{2+}-induced increase of fluorescence in nonilluminated regions. Either the proximal or the distal part of the flagellum was irradiated eight times by 8-ms UV flashes at intervals of 1 s. The change in fluorescence of Fluo-3 was measured 1 s after the last UV flash in various regions of the sperm (see legend to Fig. 7).

The MCM-esters of 8-Br-cGMP and 8-Br-cAMP have a very low absorbance at 364 nm, and therefore were photolyzed with an N_2 pulsed-laser MSG 800 (337 nm; 500 ps; Lasertechnik, Berlin, Germany). The UV light was guided onto the coverslip with fiber optics that allowed illumination of entire sperm. The sperm were UV-irradiated 10× by 500-ps flashes in intervals of 0.5 s. The fluorescence of Fluo-3 was measured 1 s after the last UV flash. To determine the decrease in fluorescence caused by bleaching the dye, the fluorescence in different regions of sperm was measured with the same protocol before and after UV irradiation without caged cyclic nucleotides. The mean difference in fluorescence, ΔF, determined from measurements of 12 different sperm, was subtracted from the increase in fluorescence measured in the presence of the caged compounds.

Results

One Short and Several Long β Subunit Transcripts are Expressed in Testis

One short and three long cDNAs encoding β subunits of CNG channels have been identified (see Materials and Methods). The three cDNAs (pCNCβ1c [3095 bp], pCNCβ1d [3102 bp], and pCNCβ1e [3302 bp]) encoding the long β subunits differ only in their 5′ends (see Fig. 1 *a* and Fig. 2). A cRNA probe (for location of probe A, see Fig. 1 *a*) specific for the 5′ terminal region of the long β subunit cDNAs, hybridized to a transcript of ~3.3 kb in testis poly(A)$^+$ RNA (Fig. 1 *b*, lane *T*, *left*), and to ~7.4 kb and ~4.4 kb transcripts in retinal poly(A)$^+$ RNA (Fig. 1 *b*, lane *R*, *left*). The retinal ~7.4-kb transcript codes for the β subunit of the CNG channel from rod photoreceptors (CNCβ1a), and the ~4.4-kb transcript for a glutamic acid–rich protein (GARP; Körschen et al., 1995). The length of the cDNAs (3095–3302 bp) is consistent with the idea that the long β subunits are encoded by the ~3.3-kb transcript(s). For pCNCβ1c and pCNCβ1e, the translational initiation sites were assigned to the first ATG triplet downstream of a nonsense codon in the same reading frame. pCNCβ1e harbors a second ATG triplet downstream of the first triplet (see Fig. 2 *c*). In contrast to the first ATG triplet, the second ATG triplet is flanked by a reasonably well-conserved Kozak sequence (GCATCATGG), and therefore represents a better translational initiation site than the first triplet. Clone pCNCβ1d does not contain a nonsense codon upstream of a putative translational initiation site; therefore, the initiation site is not certain. The deduced aa sequence of CNCβ1c consists of 938 aa with a calculated molecular mass of ~104.5; pCNCβ1e either encodes a polypeptide of 952 aa (~105.9 kD), or if the second ATG triplet is used, a polypeptide of 941 aa (~104.8 kD). Biel et al. (1996) have identified a β subunit (CNG4c) from bovine testis by cloning cDNA that differs from CNCβ1c by four aa exchanges and an additional residue.

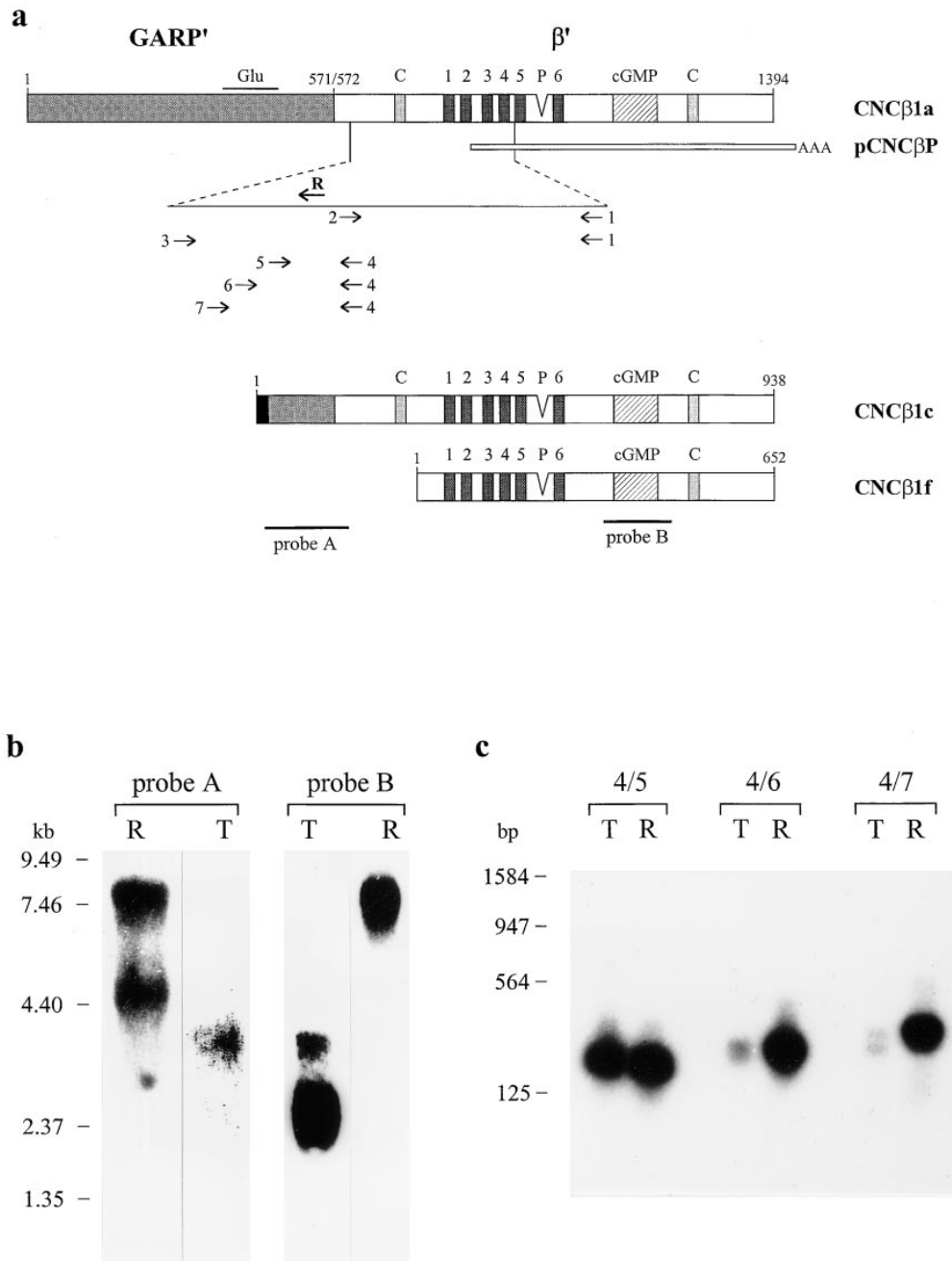

Figure 1. Cloning of β subunits and Northern blot analysis. (*a*) Schematic drawing of the primary structure of β subunits from bovine rod photoreceptor (CNCβ1a) and testis (CNCβ1c, CNCβ1f). CNCβ1a consists of a GARP part (aa 1–571) and a β′ part (aa 572–1394). The GARP part is almost identical to the bovine GARP (Sugimoto et al., 1991). Glu refers to the glutamic acid–rich region; the transmembrane segments 1–6, the cGMP-binding site (cGMP), and the calmodulin-binding sites (*C*) are depicted as boxes. P, pore region. The different 5′ ends of the long testis β subunits are represented as a black box. The COOH-terminal calmodulin-binding site does not modulate the channel activity (Grunwald et al., 1998; Weitz et al., 1998). The location of partial clone pCNCβP, and of riboprobes A and B used for Northern blot analysis is indicated. The location of primers 1–7 and primer R for 5′ RACE is shown on a larger scale below the corresponding region of CNCβ1a. (*b*) Northern blot analysis of poly(A)$^+$ RNA from bovine testis (*T*) and retina (*R*). Probe A corresponding to aa 469–578 of CNCβ1a hybridized to transcripts of ~7.4 kb and ~4.4 kb from retina and to an ~3.3-kb transcript from testis. Probe B corresponding to aa 909–1081 hybridized to transcripts of ~3.3 and 2.4 kb from testis and to an ~7.4-kb transcript from retina. Autoradiographic exposure was 3 d for testis samples and 12 h for retina samples. Integrity of poly(A)$^+$ RNA was confirmed by Northern blot analysis of transcripts encoding actin and CNCα2 (data not shown). (*c*) PCR amplification of β transcripts from testis (*T*) and retina (*R*) cDNA. Blot hybridization of PCR fragments amplified with primer pairs 4/5, 4/6, and 4/7. The blot was hybridized with a DNA probe amplified from cDNA of CNCβ1a with primer pair 4/7. Positions of size markers are given on the left-hand side.

A cRNA probe derived from the β′ part of the rod β subunit (for location of probe B see Fig. 1 *a*) in addition to the ~3.3 kb transcript recognized a transcript of ~2.4 kb in testis poly (A)$^+$ RNA (Fig. 1 *b*, lane *T*, *right*) and, as expected, the ~7.4-kb transcript in retinal poly(A)$^+$ RNA (Fig. 1 *b*, lane *R*, *right*). The hybridization signal resulting from the ~2.4-kb transcript was much stronger than that from the ~3.3-kb transcript, suggesting that at least two transcripts of different size and abundance are expressed in testis.

The 5′ end of the ~2.4-kb transcript was obtained by PCR. We used a set of primer pairs specific for the NH_2-terminal region of the β′ part of CNCβ1a to amplify 5′-located sequences (for positions of primers, see Materials and Methods and Fig. 1 *a*). Using primer pairs 1/2 and 1/3, fragments were amplified from testis cDNA that matched in size and sequence the corresponding fragments amplified from retinal cDNA. Amplification with primer pair 1/2 was significantly stronger than with primer pair 1/3 (data not shown). This result indicated that the 5′ end of an

a

CNCβ1c

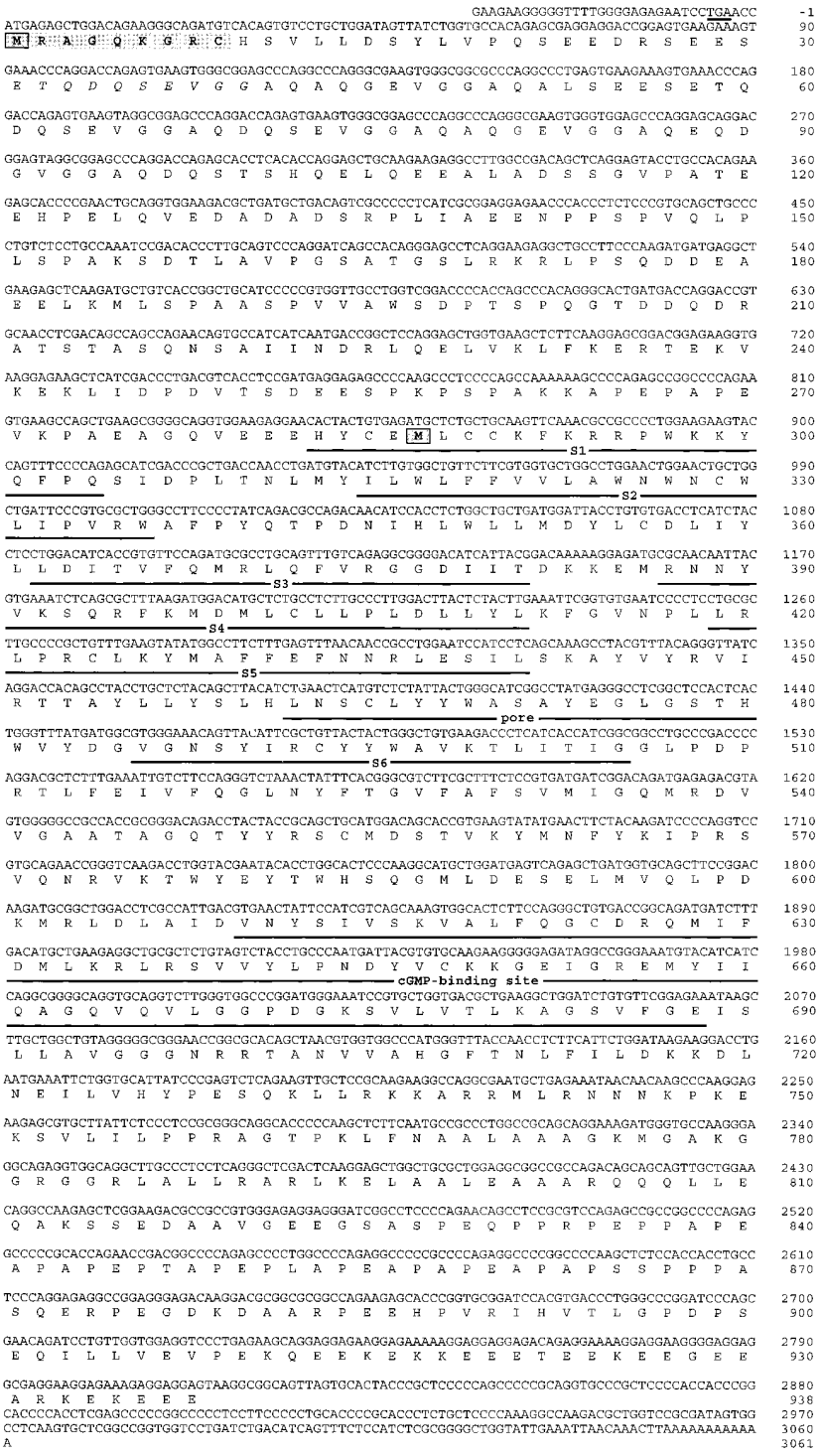

b

CNCβ1d

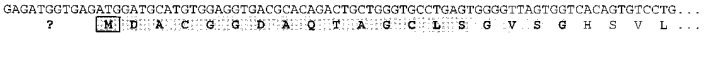

c

CNCβ1e

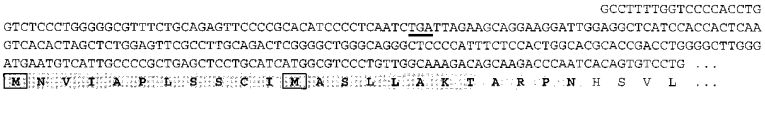

Figure 2. Nucleotide and deduced amino acid sequences of CNCβ1c/ -1d/ -1e. (*a*) Nucleotide and deduced amino acid sequence of CNCβ1c. The first nucleotide of the translational initiation codon has been assigned position +1. A nonsense codon preceding the initiation codon in the same reading frame is underlined. The initiating methionines of CNCβ1c and of the short testis β subunit (CNCβ1f) are boxed. The deduced amino acid sequence (in one-letter code) is shown below the nucleotide sequence. Amino acid residues are numbered beginning with the initiating methionine. Number of the last residue in each line is given on the right-hand side. Beginning with histidine 10 in CNCβ1c, the amino acid sequences of the three long β variants are identical. The transmembrane segments S1–S6, the pore region, and the cGMP-binding site are represented by lines above the sequence. Amino acid residues 32–40 that are missing in two of seven clones are written in italics. (*b* and *c*) Nucleotide and deduced amino acid sequences of the 5′ ends of CNCβ1d and CNCβ1e. The putative initiating methionines are boxed. Clone pCNCβ1d does not contain a nonsense codon upstream of the putative initiation codon; therefore, the initiation site is not certain (*question mark*). In pCNCβ1e, a nonsense codon preceding the initiation codon in the same reading frame is underlined. These sequence data are available from GenBank/EMBL/DDBJ under accession number AF074012 (CNCβ1c), AF074013 (CNCβ1d), AF074014 (CNCβ1e).

abundant testis transcript is located between primers 2 and 3, and that a larger transcript is much less abundant as demonstrated above by the Northern blot (Fig. 1 *b*, lane *T*, *right*). Further PCR experiments with nested primer pairs 4/5, 4/6, and 4/7 (Fig. 1 *c*) indicated that the short abundant transcript begins in the segment flanked by primers 5 and 6. The size of the cDNA ranging from this segment to the poly(dA) tail of the partial clone pCNCβP (~2.4 kbp) agrees well with the size of the short ~2.4-kb transcript, which suggests that the segment flanked by primers 5 and 6 is part of the 5′ nontranslated region of the ~2.4-kb transcript. However, this segment is part of the open reading frame in the cDNAs of the long testis β subunits. Perhaps the ~2.4-kb transcript is produced by use of an alternative promotor, as has been recently proposed for a short β transcript from human retina (Ardell et al., 1996).

The cloned cDNA of the short β subunit variant (CNCβ1f) is similar to a cDNA isolated from a human retina library (h*r*CNC2a; Chen et al., 1993; Ardell et al., 1996). Coexpression of h*r*CNC2a with the α subunit from human rod photoreceptors gives rise to functional heterooligomeric channels (Chen et al., 1993). We therefore assigned the translational initiation site of the short β subunit from testis to the corresponding triplet in h*r*CNC2a (see second boxed ATG in Fig. 2 *a*). The deduced amino acid sequence predicts a relative molecular mass of ~74.3.

The relationship between the β subunits from rod photoreceptor (CNCβ1a) and testis (CNCβ1c–f) is illustrated in Fig. 1 *a* and Fig. 2. CNCβ1a consists of a GARP part and a β′ part (Körschen et al., 1995). While the β′ part is conserved, only a small COOH-terminal region of the GARP part is left in the long variants CNCβ1c–e. The GARP part and some of the NH_2-terminal region of the β′ part (Fig. 1 *a*) are missing in CNCβ1f. The different NH_2-terminal ends of CNCβ1c–e are highlighted in Fig. 2.

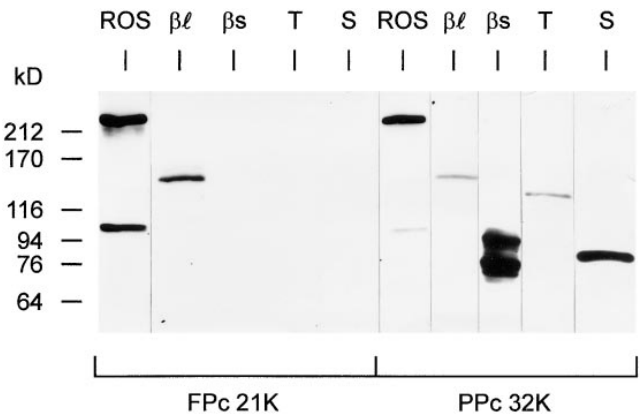

Figure 3. Western blot analysis. Western blot of heterologously expressed long (CNCβ1c) and short (CNCβ1f) testis β subunit and of membrane proteins from bovine rod outer segments, testicular tissue, and cauda epididymal sperm. The blot was probed with polyclonal antibodies FPc 21K (40 ng/ml) and PPc 32K (100 ng/ml). ROS, membranes from bovine rod outer segments (2 μg protein each); βℓ, βs: membranes from COS-1 cells transfected with cDNA encoding CNCβ1c (βℓ: 50 μg protein each); and with cDNA encoding CNCβ1f (βs: 2 μg protein each); T, membranes from testicular tissue (30 μg protein each); S, membranes from cauda epididymal sperm (30 μg protein each). In membranes of rod outer segments, FPc 21K and PPc 32K label a less abundant ~105-kD polypeptide in addition to the 240-kD β subunit (CNCβ1a). When heterologously expressed, both the long (CNCβ1c) and short (CNCβ1f) testis β subunit give rise to a doublet of polypeptides. The apparent molecular masses of the lower bands are ~150 kD (CNCβ1c) and ~76 kD (CNCβ1f). The upper bands of CNCβ1c and CNCβ1f may represent posttranslationally modified β polypeptides. Antibody FPc 21K did not label any polypeptide in sperm membranes, whereas antibody PPc 32K recognized an ~80-kD membrane protein in sperm. Molecular size standards are shown on the left-hand side.

Expression of α and β Subunits in Sperm and Precursor Cells

The low expression level of the large transcripts in testis raises the question as to what extent CNCβ1c–e are expressed in sperm or precursor cells. Translation into the respective polypeptides was examined by Western blot analysis using two different antibodies (Fig. 3). Antibody FPc 21K was raised against that NH_2-terminal region of the long β variants that is lacking in the short β form. This antibody should only recognize the long β subunits. Antibody PPc 32K was directed against an epitope in the common COOH-terminal region, and therefore should recognize all forms of β subunits. FPc 21K proved to be considerably more sensitive to β polypeptides than PPc 32K; in membranes of rod outer segments, FPc 21K stained the 240 kD β subunit and a less abundant ~105 kD isoform (see legend to Fig. 3) more intensely than did PPc 32K, although FPc 21K was used at lower concentrations (Fig. 3, compare *ROS* lanes). FPc 21K also recognized the heterologously expressed long β subunit, CNCβ1c, much better than did PPc 32K (Fig. 3, compare βℓ lanes). The heterologously expressed short testis β subunit (CNCβ1f) is not recognized by FPc 21K (Fig. 3, *left*, lane βs).

Western blot analysis of membrane proteins of cauda epididymal sperm and testis did not provide evidence for a polypeptide recognized by FPc 21K (Fig. 3, *left*, lanes *S* and *T*). This failure to detect the long β subunits may either reflect a low expression level, as suggested by the Northern blot (Fig. 1 *b*), or expression in a small subset of testicular cells (see below).

In testicular membranes, the common antibody PPc 32K recognized a weak band of ~130 kD (Fig. 3, *right*, lane *T*) that was not detected by the more sensitive antibody FPc 21K. Therefore, we interpret the labeling as an unspecific cross-reaction of PPc 32K. In contrast, in membranes of cauda epididymal sperm (Fig. 3, *right*, lane *S*) and ejaculated sperm (not shown), antibody PPc 32K intensely labeled a polypeptide of ~80 kD. The M_r is similar both to the calculated M_r and the apparent M_r of the heterologously expressed CNCβ1f (Fig. 3, *right*, lane *βs*). The occurrence of two CNCβ1f bands of ~76 and ~92 kD in transfected COS-1 cells may reflect heterogeneity due to posttranslational modifications. These results suggest, but do not prove, that the prominent ~2.4 kb transcript (see Fig. 1 *b*) encodes the short form of the β subunit.

The expression pattern of α and β subunits was examined by immunohistochemistry on testicular sections (Fig. 4) and epididymal sections (Fig. 5) using both the α subunit–specific antibody PPc 23 and the β subunit–specific antibodies FPc 21K and PPc 32K. PPc 23 and PPc 32K stained sperm and precursor cells. The staining pattern for both antibodies

varied among individual seminiferous tubules depending on the stage of spermatogenesis (Fig. 4, *a* and *b*). Antibody PPc 23 stained flagella of sperm (*arrowheads*) and granules of late spermatids (*arrows*, Fig. 4, *a* and *c*). Spermatogonia, spermatocytes, early spermatids, Sertoli cells, and intertubular cells were not labeled. The β subunit immunoreactivity obtained by PPc 32K was already detectable in spermatocytes (Fig. 4, *b* and *d*, *open arrows*). PPc 32K stained late spermatids (Fig. 4, *b* and *d, arrows*) and sperm flagella (Fig. 4 *b*, *arrowhead*) intensely. Spermatogonia, Sertoli cells, and intertubular cells were not labeled. These results suggest that β subunits are expressed earlier in development than are α subunits. The more sensitive antibody FPc 21K did not label testicular or epididymal sections (not shown). These results together with the Western blot analysis demonstrate that the expression level of the long β variants is in fact very low, and that the short β subunit is the sole physiologically relevant β variant in spermatogenic cells.

Both PPc 23 (anti-α; Fig. 5, *a* and *c*) and PPc 32K (anti-β; Fig. 5, *b* and *d*) intensely stained sperm inside the epididymal ducts. At a higher magnification, long threadlike structures were resolved that most likely represent flagella (Fig. 5 *c*). The specificity of the testicular and epididymal staining was ascertained by preincubating the primary antibody with either the respective immunogenic or with an unrelated antigen (not shown), as well as by omitting the primary antibody (Fig. 4 *e* and Fig. 5 *e*). Under these control conditions, no specific staining was detected.

Spatial Distribution of α and β Subunits in Mature Sperm

The staining patterns of epididymal sperm obtained by anti-α and anti-β antibodies differed from each other (Fig.

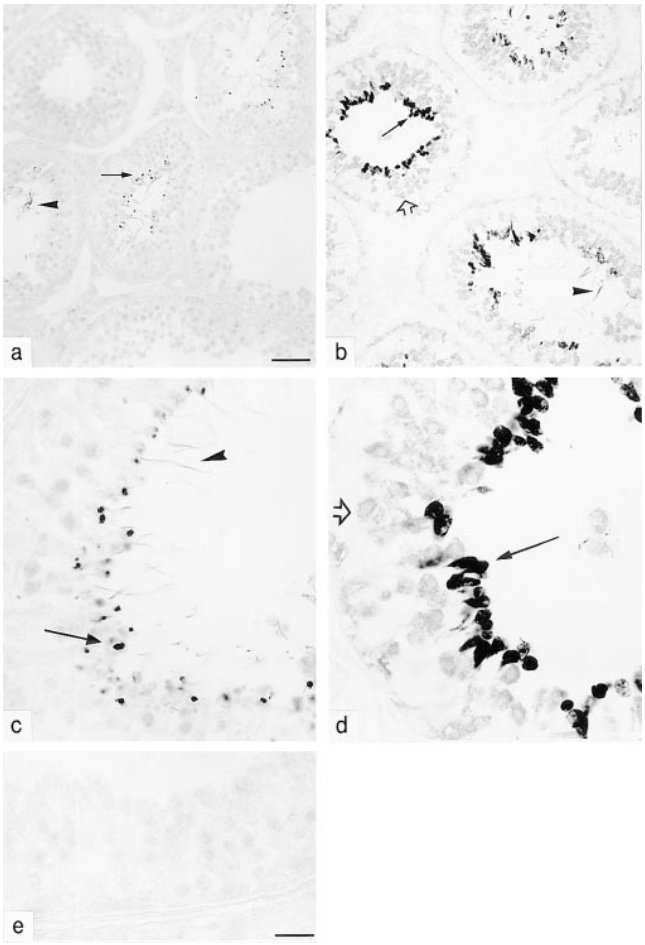

Figure 4. Immunohistochemical localization of CNG channel subunits in bovine testis. Cross-sections of seminiferous tubules were stained with antibodies specific for the α subunit (PPc 23, 3 μg/ml: *a* and *c*) and the β subunit (PPc 32K, 0.9 μg/ml: *b* and *d*) or in the absence of primary antibody (*e*). In *c*, *d*, and *e*, part of a cross-sectioned seminiferous tubule is shown. The staining pattern for both antibodies differs among individual tubules depending on the stage of spermatogenesis (*a* and *b*). The α subunit-specific antibody stained granules of late spermatids (*arrows*) and flagella (*arrowheads*). The β subunit immunoreactivity is already detectable in spermatocytes (*open arrows*); arrows denote staining of spermatids, and arrowheads denote staining of flagella. No staining is observed in the absence of primary antibody (*e*). Bars: 50 μm (*a* and *b*); 16 μm (*c–e*).

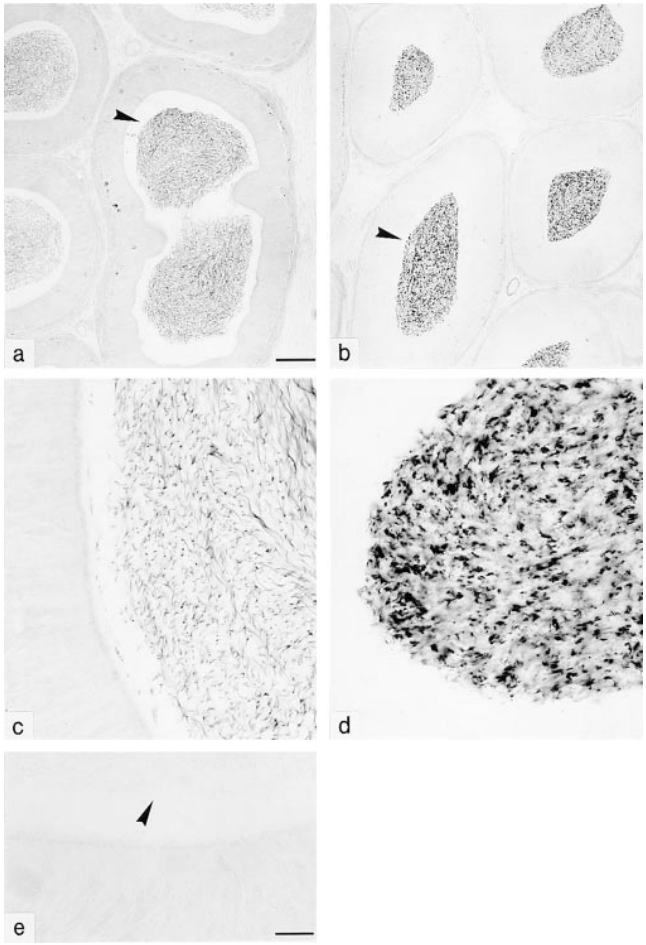

Figure 5. Immunohistochemical localization of CNG channel subunits in bovine epididymis. Epididymal cross-sections were stained with PPc 23 (*a* and *c*), PPc 32K (*b* and *d*), or in the absence of primary antibody (*e*) as in Fig. 4. In *c*, *d,* and *e* part of a cross-sectioned epididymal duct is shown. PPc 23 and PPc 32K stained sperm (*arrowheads*) inside the epididymal ducts. In the absence of primary antibody (*e*), sperm (*arrowhead*) are not labeled. Bar: 100 μm (*a* and *b*); 16 μm (*c–e*).

5, *c* and *d*), suggesting that the surface distribution of α and β subunits is different. To test this hypothesis, the spatial expression pattern of subunits was studied by immunofluorescence microscopy on isolated sperm. The α subunit–specific antibody (PPc 23) stained almost the entire flagellum of both cauda epididymal sperm (data not shown) and ejaculated sperm (Fig. 6, *a* and *c*), whereas the β subunit–specific antibody (PPc 32K) stained the proximal part of the principal piece, but not the midpiece and the distal part of the flagellum (Fig. 6, *b* and *d*). Neither PPc 23 nor the PPc 32K stained the head. As expected from the Western blot analysis (Fig. 3), FPc 21K did not stain sperm, even at concentrations that were 15× higher than those of PPc 32K (not shown). The differential expression pattern of α and β subunits along the flagellum was confirmed using the PAP/ABC method (not shown). Primary antibodies preincubated with the respective immunogenic antigen gave no staining (Fig. 6, *e* and *f*), as well as the secondary antibody alone (not shown). From these results we conclude that the α subunit is distributed along the entire flagellum, whereas the β subunit is restricted to the principal piece, suggesting that homo- and heterooligomeric forms of the CNG channel coexist in mature sperm.

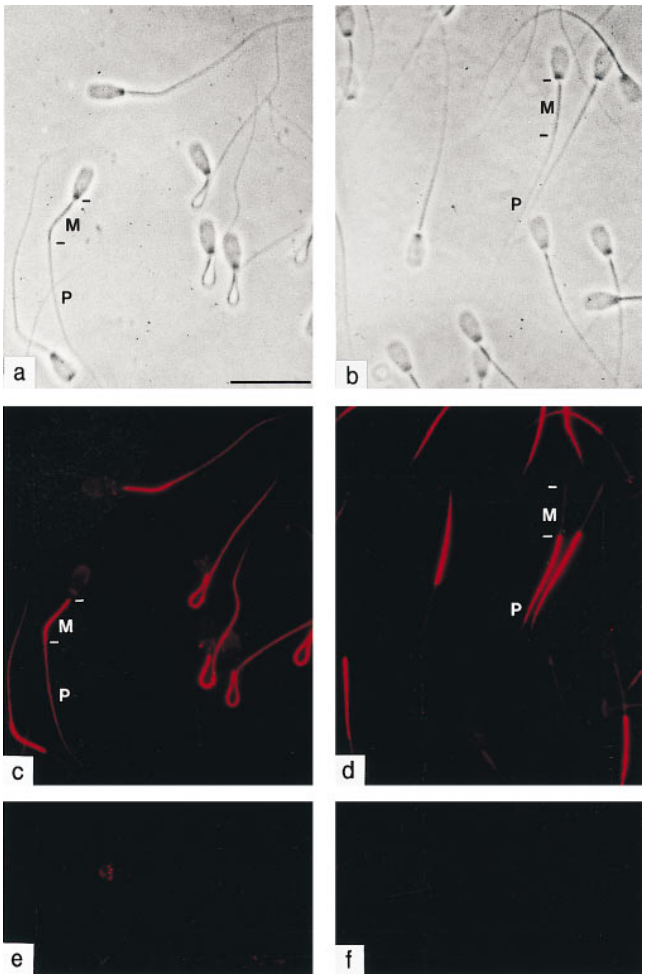

Figure 6. Immunocytochemical localization of CNG channel subunits in mature sperm. Sperm were stained with antibodies PPc 23 (1.5 μg/ml; *a* and *c*) and PPc 32K (0.3 μg/ml; *b* and *d*); (*a* and *b*) phase-contrast micrographs; (*c* and *d*) same fields in epifluorescence mode; M, midpiece; P, principal piece of the flagellum. The α subunit immunoreactivity is detectable along almost the entire flagellum (*c*), whereas the β subunit immunoreactivity is restricted to the proximal part of the principal piece (*d*). Preincubation of the primary antibodies with the respective immunogenic antigen abolished the specific staining (*e* and *f*). Bar, 20 μm.

CNG Channel-mediated Ca^{2+} Influx Into Sperm

Owing to their substantial Ca^{2+} permeability, CNG channels are prime candidates for mediating Ca^{2+} entry into sperm. We investigated Ca^{2+} entry into sperm using confocal laser scanning microscopy (CLSM) in conjunction with the Ca^{2+} indicator Fluo-3 and novel caged cyclic nucleotides. The combination of high-resolution CLSM with fast and selective liberation of cyclic nucleotide analogues made it possible to demonstrate for the first time CNG channel–mediated Ca^{2+} influx into sperm.

Sperm loaded with Fluo-3 did not fluoresce uniformly at rest (Fig. 7 *A*). The Fluo-3 fluorescence was stronger in the acrosomal region and in some local areas of the midpiece where mitochondria are located. This finding suggests that the basal $[Ca^{2+}]_i$ is higher in the acrosomal vesicle and in mitochondria than in other cell compartments, consistent with the idea that these organelles serve as intracellular Ca^{2+} stores (Irvine and Aitken, 1986; Meizel and Turner, 1993).

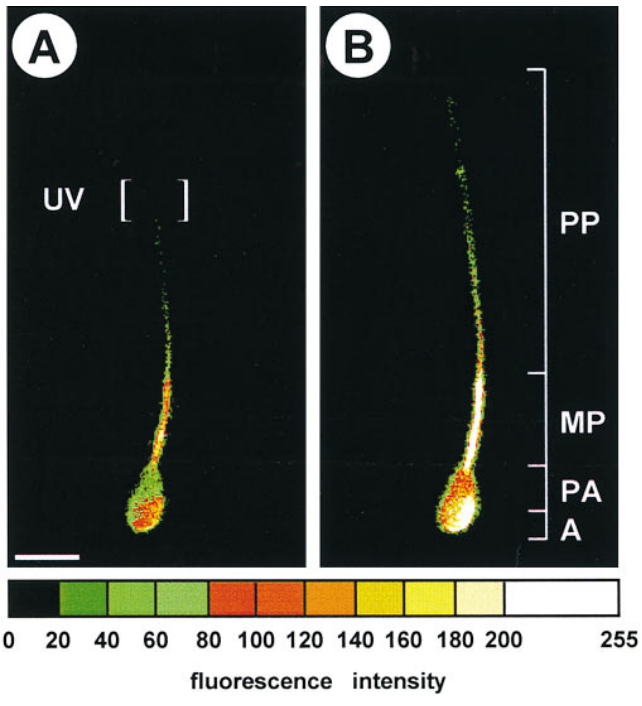

Figure 7. Ca^{2+} imaging of a bovine sperm cell. Fluorescence intensity of the calcium indicator dye, Fluo-3, before (*A*) and after (*B*) liberation of 8-pCPT-cGMP from DMNB 8-pCPT-cGMP (10 μM). Fluorescence intensities are indicated by an artificial color code. The part of the sperm flagellum that was illuminated by UV light is indicated. A, acrosomal region; PA, postacrosomal region; MP, midpiece; PP, principal piece. Bar, 7.5 μm.

Photolysis of both 4,5-dimethoxy-2-nitrobenzyl (DMNB) 8-Br-cGMP (Hagen et al., 1996) and DMNB 8-pCPT-cGMP by UV light evoked a Ca^{2+} influx into sperm in 88% of the cells (n = 209/237). Because 8-pCPT-derivatives of cyclic nucleotides cross membranes more readily than do 8-Br-derivatives (Butt et al., 1992), DMNB 8-pCPT-cGMP was used to investigate the Ca^{2+} influx in more detail by illuminating either the proximal or the distal region of the principal piece (see Materials and Methods and Fig. 7). In the absence of caged 8-pCPT-cGMP, no change in fluorescence was observed in response to a UV flash (Fig. 8, *UV*). This control experiment showed that the increase of $[Ca^{2+}]_i$ did not arise from UV-induced damage of the plasma membrane, but was due to liberation of 8-pCPT-cGMP from the caged compound. In the presence of 2 mM extracellular Ca^{2+}, photoreleased 8-pCPT-cGMP evoked an increase of $[Ca^{2+}]_i$ in the acrosomal (*A*) and postacrosomal (*PA*) region of the head, in the midpiece (*MP*), and in the principal piece (*PP)* of the flagellum (Fig. 8, Ca^{2+}). No increase of $[Ca^{2+}]_i$ was detected when the extracellular solution contained no Ca^{2+} and 500 μM EGTA (Fig. 8, 0 Ca^{2+}). These results demonstrate that the $[Ca^{2+}]_i$ increase was caused by Ca^{2+} influx from outside rather than by a release from intracellular Ca^{2+} stores.

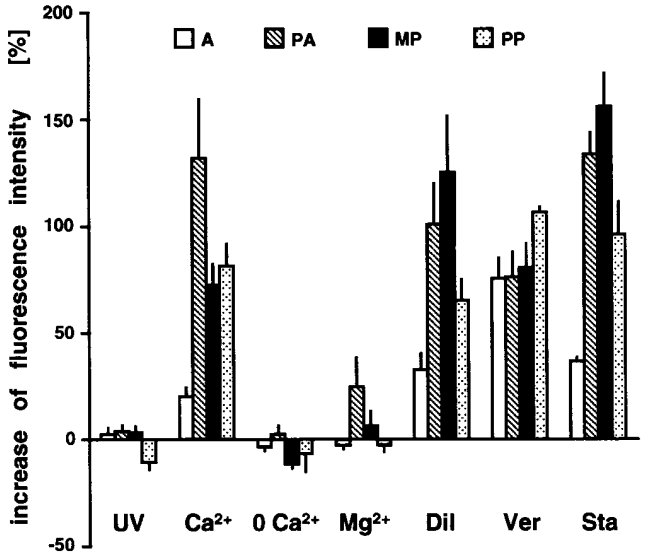

regions	UV	Ca^{2+}	0 Ca^{2+}	Mg^{2+}	Dil	Ver	Sta
A	8	10	9	9	11	9	8
PA	8	14	13	12	10	9	7
MP	9	16	11	13	9	11	7
PP	9	15	9	11	9	10	6

Figure 8. Increase of fluorescence intensity in sperm after photolysis of caged 8-pCPT-cGMP. Sperm were incubated with 10 μM DMNB 8-pCPT-cGMP. The increase of fluorescence (mean ± SEM) in various regions (for abbreviations see Fig. 7) of sperm was determined at the following conditions (extracellular concentrations in mM): UV: 2 Ca^{2+}, no DMNB 8-pCPT-cGMP; Ca^{2+}: 2 Ca^{2+}; 0 Ca^{2+}: no Ca^{2+}, 0.5 EGTA; Mg^{2+}: 2 Ca^{2+}, 15 Mg^{2+}; Dil: 2 Ca^{2+}, 0.025 D-*cis*-diltiazem; Ver: 2 Ca^{2+}, 0.0025 verapamil; Sta: 2 Ca^{2+}, 0.001 staurosporine. Number of analyzed regions is given in the chart.

A characteristic property of CNG channels is their blockage by extracellular Mg^{2+} (Weyand et al., 1994; Frings et al., 1995). The 8-pCPT-cGMP–induced Ca^{2+} influx into sperm is almost entirely suppressed by 15 mM extracellular Mg^{2+} (Fig. 8, Mg^{2+}). Such a $[Mg^{2+}]$ is not expected to block Ca^{2+} currents through voltage-activated Ca^{2+} channels (McDonald et al., 1994). Furthermore, sperm preincubated with high concentrations of blockers for voltage-activated Ca^{2+} channels (25 μM D-*cis*-diltiazem; 2.5 μM verapamil) did respond with an increase of $[Ca^{2+}]_i$ to UV light (Fig. 8, Dil, Ver). High concentration (1 μM) of staurosporine, an inhibitor of cyclic nucleotide-dependent kinases, did not suppress the 8-pCPT-cGMP–induced increase of $[Ca^{2+}]_i$ (Fig. 8, Sta). These results rule out the possibility that 8-pCPT-cGMP activates a Ca^{2+} conductance indirectly by means of a protein kinase G–mediated phosphorylation. In conclusion, we interpret these results to indicate that the Ca^{2+} influx is due to activation of CNG channels.

Ca^{2+} Influx Into Sperm is More Sensitive to cGMP Than to cAMP

Although the heterologously expressed α subunit from testis is ~200-fold more sensitive to cGMP than to cAMP, in the native channel consisting of α and β subunits, the ligand selectivity may be changed. Therefore, we investigated whether cGMP and cAMP differ in their efficacy to evoke a Ca^{2+} influx into sperm. We used two novel caged compounds—MCM 8-Br-cGMP and MCM 8-Br-cAMP—that differ only marginally in their aqueous solubilities (≤100 μM) and their photolytic quantum yields (Hagen et al., manuscript in preparation). Therefore, differences between these compounds in their efficacy to evoke a Ca^{2+} influx must be attributed to a difference in their apparent ligand affinity for the CNG channel.

Fig. 9 shows the increase of fluorescence intensity in sperm at various concentrations of either MCM 8-Br-cGMP or MCM 8-Br-cAMP. Over a large concentration range of MCM 8-Br-cAMP (10^{-6}–10^{-4} M), a small progressive increase of $[Ca^{2+}]_i$ was detected after liberating 8-Br-cAMP. In contrast, photolysis of MCM 8-Br-cGMP induced much larger increases of $[Ca^{2+}]_i$ than did MCM 8-Br-cAMP at the respective concentrations. For example, at 100 μM, photolysis of MCM 8-Br-cGMP produced a six- to sevenfold increase of fluorescence intensity in the principal piece (PP), whereas photolysis of MCM 8-Br-cAMP increased the fluorescence intensity only ~1.8-fold. Although these experiments do not allow an estimate of the apparent ligand sensitivity of the native channel, the higher efficacy of 8-Br-cGMP to increase $[Ca^{2+}]_i$ compared with 8-Br-cAMP agrees well with the high selectivity of the heterologously expressed α subunit for cGMP compared with cAMP. These findings suggest that native CNG channels represent the target of a cGMP-signaling pathway that controls Ca^{2+} entry into sperm.

Discussion

We have provided evidence that CNG channels are located on the flagellum and serve as a Ca^{2+} entry pathway

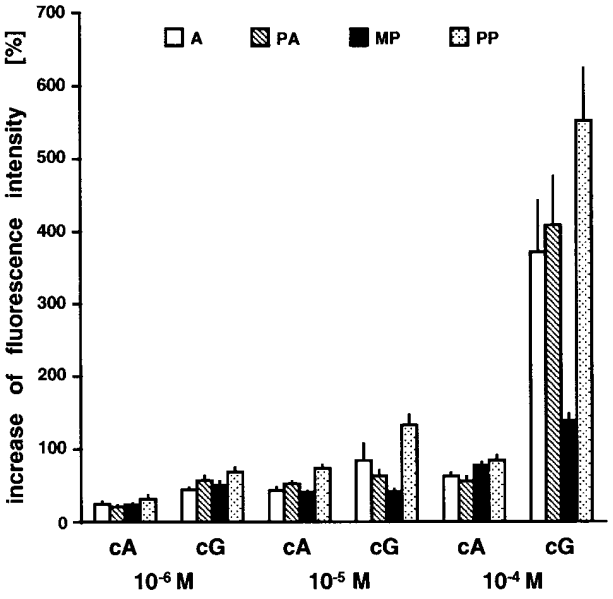

regions	cA 10^{-6}	cG 10^{-6}	cA 10^{-5}	cG 10^{-5}	cA 10^{-4}	cG 10^{-4}
A	13	17	15	15	13	10
PA	11	17	15	15	12	14
MP	13	17	15	15	13	12
PP	10	17	16	15	9	13

Figure 9. Increase of fluorescence intensity in sperm after photolysis of caged 8-Br-cGMP and caged 8-Br-cAMP. Sperm were incubated with MCM 8-Br-cAMP (*cA*) or MCM 8-Br-cGMP (*cG*; 10^{-4}, 10^{-5}, 10^{-6} M each). The increase of fluorescence (mean ± SEM) in regions (for abbreviations see Fig. 7) of sperm was determined in the presence of 2 mM extracellular Ca^{2+}. Number of analyzed regions is given in the chart. The differences between the fluorescence intensities obtained at 10^{-4} M cA and 10^{-4} M cG are statistically significant ($P < 0.05$, unpaired *t* test).

in sperm. The dissimilar expression of α and β subunits along the flagellum suggests that homo- and heterooligomeric channels coexist in vivo. The physiological implications of these findings are addressed in the following discussion.

Testicular β Subunits

A short (~2.4 kb) and several long (~3.3 kb) less abundant transcripts of the β subunit are expressed in testis. Western blotting and immunocytochemistry failed to detect long β subunits in sperm as well as in testicular precursor cells; therefore, these subunit species must be expressed at a rather low level if at all.

The 80-kD β subunit (CNCβ1f) expressed in sperm is probably encoded by the ~2.4-kb transcript. Although we were unable to identify unequivocally the 5′ nontranslated region of the ~2.4-kb transcript, both the short β clone and a similar β clone isolated from a human retinal library (Chen et al., 1993; Ardell et al., 1996) produce functional polypeptides in a cell line (Chen et al., 1993; J. Weiner and F. Müller, unpublished data). Whether the ~2.4-kb transcript is generated by use of an alternative promotor as recently proposed for the short β transcript from human retina (Ardell et al., 1996), is not known. However, genes that are expressed in testis and other tissues often give rise to testis-specific transcripts that are generated by using testis-specific promotors, altered polyadenylation, and alternative exon splicing (Erikson, 1990).

CNCβ1f is lacking the entire GARP part and a significant NH_2-terminal portion of the β′ part of the rod β subunit (CNCβ1a). An unconventional CaM-binding site that exists in this NH_2-terminal region of CNCβ1a (see Fig. 1 *a*) controls ligand sensitivity (Grunwald et al., 1998; Weitz et al., 1998). The decrease of the apparent ligand sensitivity by Ca^{2+}/CaM in rod photoreceptors has been proposed to represent a feedback mechanism that terminates the light response and participates in the recovery process after stimulation (for review see Molday, 1996). The NH_2-terminal CaM-binding site is absent in CNCβ1f. Therefore, potential modulation of the sperm CNG channel by Ca^{2+}/CaM cannot occur through the β subunit. The sperm α subunit contains in its NH_2-terminal region a segment that is highly homologous to a conventional CaM-binding site that is also present in the α subunit of olfactory CNG channels. However, no modulation by Ca^{2+}/CaM was observed for human and bovine CNCα2 channels (Yu et al., 1996; Bönigk et al., 1996; for another review see Biel et al., 1996). Gordon and coworkers (1995) provided some evidence that an unknown Ca^{2+}-dependent factor, in addition to or instead of CaM, may control CNG channel activity in rod photoreceptors. An unknown factor may also control activtity of the sperm CNG channel. Expression of CNCβ1f in sperm may be physiologically important. Sperm contain sizeable amounts of CaM, and Ca^{2+}/CaM-dependent activation of axonemal proteins play a crucial role in regulating motility (for review see Tash, 1990). Lack of CaM-binding sites in CNCβ1f may reflect a specific cellular adjustment to preclude a Ca^{2+}/CaM-dependent regulation of CNG channel activity in sperm, and perhaps expression of a short β form ensures that the channel is specifically modulated by its cognate modulatory factor.

Physiological Implications of Differential Distribution of cGMP-gated Channel Forms

A significant finding of this study concerns the cGMP-specific Ca^{2+} influx into sperm through CNG channels. Numerous studies have emphasized the importance of cAMP as an internal messenger in vertebrate sperm, whereas cGMP has been considered an orphan molecule. For example, a rise in cAMP has been proposed to promote phosphorylation of flagellar proteins by protein kinase A, thereby regulating sperm motility (Tash, 1990). The cGMP levels in vertebrate sperm are low (Gray et al., 1976), and neither a membrane-bound nor a soluble guanylyl cyclase have been convincingly identified. The presence of a CNG channel that is considerably more sensitive to cGMP than to cAMP strongly argues for a physiological function of cGMP as signaling molecule in vertebrate sperm. Furthermore, exclusive localization of the CNG channel in the flagellum favors a role in the regulation of motility rather than in the control of acrosomal exocytosis. However, high concentrations of cGMP (or cAMP) may

evoke an elevation of $[Ca^{2+}]_i$ that is propagated to the head. This increase of $[Ca^{2+}]_i$ could eventually induce acrosomal exocytosis.

The sperm surface is divided into distinct domains, each characterized by a specific protein inventary (Myles et al., 1981; Cowan and Myles, 1993). The segmental distribution of α and β subunits along the flagellum nicely fits the idea of a sectorial organization of the flagellum. In particular, the areas of subunit expression coincide with the segmentation of flagellum based on morphological criteria. While the midpiece and the distal part of the principal piece harbor only the α polypeptide, the proximal part of the principal piece harbors α and β polypetides. These results suggest that CNG channels coexist as homo- and heterooligomers in vivo, although we can not rigorously preclude that additional as yet unknown subunits participate in the formation of heterooligomeric complexes.

The dissimilar distribution of α and β polypeptides along the flagellum may have important physiological implications. The pore region located between transmembrane segments S5 and S6 of all α subunits comprises a negatively charged glutamate or aspartate residue that is crucially important for ionic selectivity, gating, and channel blockage by extracellular Ca^{2+}(Root and MacKinnon, 1993; Eismann et al., 1994; Sesti et al., 1995). This residue is replaced by a glycine residue in the pore region of β subunits. As expected, both Ca^{2+} blockage and ionic selectivity of heterooligomeric rod channels (consisting of α and β subunits) are different from those of homooligomeric α subunits (Körschen et al., 1995). Similarly, the homooligomeric α subunit cloned from testis (CNCα2) and heterooligomeric channels (CNCα2 + CNCβ1c) differ markedly in their blockage by extracellular Ca^{2+} (J. Weiner and R. Seifert, unpublished results). It is plausible that the β subunit also modifies Ca^{2+} permeability, although that has not yet been experimentally demonstrated. If so, a regional expression of CNG channel subtypes with different Ca^{2+} permeability is expected to create Ca^{2+} microdomains. Tuning $[Ca^{2+}]_i$ along the flagellum may provide a molecular basis for regulating sperm motility. In fact, the behavioral response of sperm induced by chemoattractive factors depends on external Ca^{2+}, as has been shown for a variety of invertebrates (for review see Cosson, 1990). Moreover, oscillating changes in $[Ca^{2+}]_i$ occur in hamster sperm during hyperactive motility (Suarez et al., 1993).

This study provides the first evidence that motility of sperm may be regulated by Ca^{2+} entry through CNG channels. It will be crucially important for future work to examine whether uneven distribution of CNG channel subtypes in fact gives rise to a spatiotemporal pattern of flagellar $[Ca^{2+}]$. Moreover, it needs to be shown that this pattern provides the molecular basis for modulating sperm swimming behavior.

We thank Drs. A. Baumann, W. Bönigk, J.E. Brown, E. Eismann, S. Frings, and H.G. Körschen for critical reading of the manuscript, H.G. Körschen for the gift of antibodies, and S. Gotzes for testing antibodies on retinal sections. We thank M. Bruns, B. Gentsch, M. Jetten, J. Lossmann, and B. Oczko for technical assistance, and A. Eckert for preparing the manuscript. We express our gratitude to Dr. K.-H. Wrobel (Regensburg) and Dr. M. Davidoff (Hamburg) for helpful comments on the immunohistochemistry of bovine testis, and we acknowledge a gift of ejaculated bull sperm by Dr. A. Görlach (Kleve).

This work was supported by grants from the Deutsche Forschungsgemeinschaft to I. Weyand and V. Hagen and the Ministerium für Wissenschaft und Forschung des Landes Nordrhein-Westfalen to U.B. Kaupp.

Received for publication 30 December 1996 and in revised form 5 June 1998.

References

Ardell, M.D., I. Aragon, L. Oliveira, G.E. Porche, E. Burke, and S.J. Pittler. 1996. The β subunit of human rod photoreceptor cGMP-gated cation channel is generated from a complex transcription unit. *FEBS Lett.* 389:213–218.

Arnoult, C., Y. Zeng, and H.M. Florman. 1996. ZP3-dependent activation of sperm cation channels regulates acrosomal secretion during mammalian fertilization. *J.Cell Biol.* 134:637–645.

Aviv, H., and P. Leder. 1972. Purification of biologically active globin messenger RNA by chromatography on oligothymidylic acid-cellulose. *Proc. Natl. Acad. Sci. USA.* 69:1408–1412.

Biel, M., X. Zong, A. Ludwig, A. Sautter, and F. Hofmann. 1996. Molecular cloning and expression of a modulatory subunit of the cyclic nucleotide-gated cation channel. *J. Biol. Chem.* 271:6349–6355.

Bönigk, W., F. Müller, R. Middendorff, I. Weyand, and U.B. Kaupp. 1996. Two alternatively spliced forms of the cGMP-gated channel α-subunit from cone photoreceptor are expressed in the chick pineal organ. *J. Neurosci.* 16:7458–7468.

Bradley, J., J. Li, N. Davidson, H.A. Lester, and K. Zinn. 1994. Heteromeric olfactory cyclic nucleotide-gated channels: A new subunit that confers increased sensitivity to cAMP. *Proc. Natl. Acad. Sci. USA.* 91:8890–8894.

Butt, E., C. Nolte, S. Schulz, J. Beltman, J.A. Beavo, B. Jastorff, and U. Walter. 1992. Analysis of the functional role of cGMP-dependent protein kinase in intact human platelets using a specific activator 8-*para*-chlorophenylthio-cGMP. *Biochem. Pharmacol.* 43:2591–2600.

Chen, C., and H. Okayama. 1987. High-efficiency transformation of mammalian cells by plasmid DNA. *Mol. Cell. Biol.* 7:2745–2752.

Chen, T.-Y., Y.-W. Peng, R.S. Dhallan, B. Ahamed, R.R. Reed, and K.-W. Yau. 1993. A new subunit of the cyclic nucleotide-gated cation channel in retinal rods. *Nature.* 362:764–767.

Chirgwin, J.M., A.E. Przybyla, R.J. MacDonald, and W.J. Rutter. 1979. Isolation of biologically active ribonucleic acid from sources enriched in ribonuclease. *Biochemistry.* 18:5294–5299.

Cohen-Dayag, A., I. Tur-Kaspa, J. Dor, S. Mashiach, and M. Eisenbach. 1995. Sperm capacitation in humans is transient and correlates with chemotactic responsiveness to follicular factors. *Proc. Natl. Acad. Sci. USA.* 92:11039–11043.

Cook, S.P., C.J. Brokaw, C.H. Muller, and D.F. Babcock. 1994. Sperm chemotaxis: egg peptides control cytosolic calcium to regulate flagellar responses. *Dev. Biol.* 165:10–19.

Cosson, M.P. 1990. Sperm chemotaxis. *In* Controls of Sperm Motility: Biological and Clinical Aspects. C. Gagnon, editor. CRC Press, Boca Raton, FL. 103–135.

Cowan, A.E., and D.G. Myles. 1993. Biogenesis of surface domains during spermiogenesis in the guinea pig. *Dev. Biol.* 155:124–133.

Eismann, E., F. Müller, S.H. Heinemann, and U.B. Kaupp. 1994. A single negative charge within the pore region of a cGMP-gated channel controls rectification, Ca^{2+} blockage and ionic selectivity. *Proc. Natl. Acad. Sci. USA.* 91: 1109–1113.

Erickson, R.P. 1990. Post-meiotic gene expression. *Trends Genet.* 6:264–269.

Finn, J.T., M.E. Grunwald, and K.-W. Yau. 1996. Cyclic nucleotide-gated ion channels: an extended family with diverse functions. *Annu. Rev. Physiol.* 58: 395–426.

Frings, S., R. Seifert, M. Godde, and U.B. Kaupp. 1995. Profoundly different calcium permeation and blockage determine the specific function of distinct cyclic nucleotide-gated channels. *Neuron.* 15:169–179.

Frohman, M.A., M.K. Dush, and G.R. Martin. 1988. Rapid production of full-length cDNAs from rare transcripts: amplification using a single gene-specific oligonucleotide primer. *Proc. Natl. Acad. Sci. USA.* 85:8998–9002.

Garbers, D.L. 1989. Molecular basis of fertilization. *Annu. Rev. Biochem.* 58: 719–742.

Gordon, S.E., J. Downing-Park, and A.L. Zimmerman. 1995. Modulation of the cGMP-gated ion channel in frog rods by calmodulin and an endogenous inhibitory factor. *J. Physiol.* 486:533–546.

Gordon, S.E., J.C. Oakley, M.D. Varnum, and W.N. Zagotta. 1996. Altered ligand specificity by protonation in the ligand binding domain of cyclic nucleotide-gated channels. *Biochemistry.* 35:3994–4001.

Gray, J.P., G.I. Drummond, D.W.T. Luk, J.G. Hardman, and E.W. Sutherland. 1976. Enzymes of cyclic nucleotide metabolism in invertebrate and vertebrate sperm. *Arch. Biochem. Biophys.* 172:20–30.

Grunwald, M.E., W.-P. Yu, H.-H. Yu, and K.-W. Yau. 1998. Identification of a domain on the β-subunit of the rod cGMP-gated cation channel that mediates inhibition by calcium-calmodulin. *J. Biol. Chem.* 273:9148–9157.

Hagen, V., C. Dzeja, S. Frings, J. Bendig, E. Krause, and U.B. Kaupp. 1996. Caged compounds of hydrolysis-resistant analogues of cAMP and cGMP: Synthesis and application to cyclic nucleotide-gated channels. *Biochemistry.* 35:7762–7771.

Hansbrough, J.R., and D.L. Garbers. 1981. Speract - Purification and character-

ization of a peptide associated with eggs that activates spermatozoa. *J. Biol. Chem*. 256:1447–1452.
Harper, M.J.K. 1994. Gamete and zygote transport. *In* The Physiology of Reproduction. Vol. 1. E. Knobil and J.D. Neill, editors. Raven Press Ltd., New York. 123–187.
Irvine, D.S., and R.J. Aitken. 1986. Measurement of intracellular calcium in human spermatozoa. *Gamete Res*. 15:57–71.
Kaupp, U.B. 1995. Family of cyclic nucleotide gated ion channels. *Curr. Opin. Neurobiol*. 5:434–442.
Körschen, H.G., M. Illing, R. Seifert, F. Sesti, A. Williams, S. Gotzes, C. Colville, F. Müller, A. Dosé, M. Godde, et al. 1995. A 240 kDa protein represents the complete β subunit of the cyclic nucleotide-gated channel from rod photoreceptor. *Neuron.* 15:627–636.
Liman, E.R., and L.B. Buck. 1994. A second subunit of the olfactory cyclic nucleotide-gated channel confers high sensitivity to cAMP. *Neuron.* 13:611–621.
McDonald, T.F., S. Pelzer, W. Trautwein, and D.J. Pelzer. 1994. Regulation and modulation of calcium channels in cardiac, skeletal, and smooth muscle cells. *Physiol. Rev*. 74:365–507.
Meizel, S., and K.O. Turner. 1993. Initiation of the human sperm acrosome reaction by thapsigargin. *J. Exp. Zool*. 267:350–355.
Middendorff, R., E. Maronde, H.-J. Paust, D. Müller, M. Davidoff, and J. Olcese. 1996. Expression of C-type natriuretic peptide in the bovine pineal gland. *J. Neurochem*. 67:517–524.
Molday, R.S. 1996. Calmodulin regulation of cyclic-nucleotide-gated channels. *Curr. Opin. Neurobiol*. 6:445–452.
Myles, D.G., P. Primakoff, and A.R. Bellvé. 1981. Surface domains of the guinea pig sperm defined with monoclonal antibodies. *Cell.* 23:433–439.
Ralt, D., M. Goldenberg, P. Fetterolf, D. Thompson, J. Dor, J. Mashiach, D.L. Garbers, and M. Eisenbach. 1991. Sperm attraction to a follicular factor(s) correlates with human egg fertilizability. *Proc. Natl. Acad. Sci. USA*. 88: 2840–2844.
Root, M.J., and R. MacKinnon. 1993. Identification of an external divalent cation-binding site in the pore of a cGMP-activated channel. *Neuron.* 11:459–466.
Rotem, R., N. Zamir, N. Keynan, D. Barkan, H. Breitbart, and Z. Naor. 1998. Atrial natriuretic peptide induces acrosomal exocytosis of human spermatozoa. *Am. J. Physiol*. 274:E218–E223.
Santos-Sacchi, J., and M. Gordon. 1980. Induction of the acrosome reaction in guinea pig spermatozoa by cGMP analogues. *J.Cell Biol.* 85:798–803.
Sautter, A., X. Zong, F. Hofmann, and M. Biel. 1998. An isoform of the rod photoreceptor cyclic nucleotide-gated channel β subunit expressed in olfactory neurons. *Proc. Natl. Acad. Sci. USA*. 95:4696–4701.
Schackmann, R.W., and P.B. Chock. 1986. Alteration of intracellular [Ca^{2+}] in sea urchin sperm by the egg peptide speract. *J. Biol. Chem*. 261:8719–8728.
Sesti, F., E. Eismann, U.B. Kaupp, M. Nizzari, and V. Torre. 1995. The multiion nature of cGMP-gated channel from vertebrate rods. *J. Physiol.* 487:17–36.
Suarez, S.S., S.M. Varosi, and X. Dai. 1993. Intracellular calcium increases with hyperactivation in intact, moving hamster sperm and oscillates with the flagellar beat cycle. *Proc. Natl. Acad. Sci. USA.* 90:4660–4664.
Sugimoto, Y., K. Yatsunami, M. Tsujimoto, H.G. Khorana, and A. Ichikawa. 1991. The amino acid sequence of a glutamic acid-rich protein from bovine retina as deduced from the cDNA sequence. *Proc. Natl. Acad. Sci. USA*. 88: 3116–3119.
Tash, J.S. 1990. Role of cAMP, calcium, and protein phosphorylation in sperm motility. *In* Controls of Sperm Motility: Biological and Clinical Aspects. C. Gagnon, editor. CRC Press, Boca Raton, FL. 229–240.
Ward, C.R., and G.S. Kopf. 1993. Molecular events mediating sperm activation. *Dev. Biol*. 158:9–34.
Ward, G.E., C.J. Brokaw, D.L. Garbers, and V.D. Vacquier. 1985. Chemotaxis of *Arbacia punctulata* spermatozoa to resact, a peptide from the egg jelly layer. *J. Cell Biol*. 101:2324–2329.
Weitz, D., M. Zoche, F. Müller, M. Beyermann, H.G. Körschen, U.B. Kaupp, and K.-W. Koch. 1998. Calmodulin controls the rod photoreceptor CNG channel through an unconventional binding site in the N-terminus of the β-subunit. *EMBO (Eur. Mol. Biol. Organ.) J*. 17:2273–2284.
Weyand, I., M. Godde, S. Frings, J. Weiner, F. Müller, W. Altenhofen, H. Hatt, and U.B. Kaupp. 1994. Cloning and functional expression of a cyclic-nucleotide-gated channel from mammalian sperm. *Nature.* 368:859–863.
Yu, W.-P., M.E. Grunwald, and K.-W. Yau. 1996. Molecular cloning, functional expression and chromosomal localization of a human homolog of the cyclic nucleotide-gated ion channel of retinal cone photoreceptor. *FEBS Lett*. 393: 211–215.
Záborszky, L., and C. Léránth. 1985. Simultaneous ultrastructural demonstration of retrogradelly transported horseradish peroxidase and choline acetyltransferase immunoreactivity. *Histochemistry.* 82:529–537.